IEEE Access
Multidisciplinary | Rapid Review | Open Access Journal

Received April 21, 2020, accepted April 29, 2020, date of publication May 4, 2020, date of current version May 19, 2020.

Digital Object Identifier 10.1109/ACCESS.2020.2992338

Bayesian Cooperative Localization With NLOS and Malicious Vehicle Detection in GNSS-Challenged Environments

JUNHUI ZHAO[1,2], (Senior Member, IEEE), YINGHAO ZHANG[2], SHANJIN NI[2], AND QIUPING LI[2]

[1]School of Information Engineering, East China Jiaotong University, Nanchang 330013, China
[2]School of Electronic and Information Engineering, Beijing Jiaotong University, Beijing 100044, China

Corresponding author: Junhui Zhao (junhuizhao@hotmail.com)

This work was supported in part by the National Natural Science Foundation of China under Grant 61971191 and Grant 61661021, in part by the Beijing Natural Science Foundation under Grant L182018, in part by the National Science and Technology Major Project of the Ministry of Science and Technology of China under Grant 2016ZX03001014-006, and in part by the Open Research Fund of the National Mobile Communications Reasearch Laboratory, Southeast University under Grant 2017D14.

ABSTRACT Owing to the inter-vehicle non-line-of-sight (NLOS) measurement and malicious attack in global navigation satellite system (GNSS) challenged environment, the vehicle position precision is seriously damaged. In order to improve the vehicle position accuracy, we propose a new Bayesian cooperative localization scheme which tackles this problem by combining the vehicle position measurements and inter-vehicle distance measurements. In the proposed scheme, an abnormal vehicle detection algorithm (AVDA) is presented to eliminate the impacts of NLOS and malicious attack. Simulation results demonstrate that the proposed scheme can achieve excellent localization performance in the presence of NLOS and malicious attacks. Based on these results, the abnormal and normal detection rates of AVDA are approximate and the root mean square error (RMSE) is reduced to the sub-meter level. The performances of the proposed scheme are also verified in real environmental conditions by using the simulation of urban mobility (SUMO).

INDEX TERMS Bayesian cooperative localization, inter-vehicle distance, malicious attack, NLOS, VANET.

I. INTRODUCTION

Intelligent transportation systems (ITS), which aims at providing innovative services and making safer, more convenient use of traffic network, typically depends on the accurate and reliable vehicle location information [1]. Currently, the Global Navigation Satellite System (GNSS) plays an important role in acquiring the vehicle location information [2]. Through some enhancement technologies [3], [4], the GNSS has the capability to achieve the meter level accuracy, even the centimeter level. However, due to the faded or blocked GNSS signals, the validity of these GNSS systems is limited by the complex local environmental conditions [5]. In order to solve this problem, the cooperative localization approach is introduced. The cooperation in vehicular networking is able to alleviate the shortcomings of GNSS by incorporating the additional information which is independent of GNSS [6]. With the assistant of the emerging technologies in the fifth generation (5G) mobile cellular systems [7], [8] and the vehicle ad-hoc network (VANET) [9], [10], vehicles are allowed to establish a connection with each other, which supports to implement cooperative localization technology within vehicular networking. Cooperative localization in VANET exchanges the measurements of vehicle nodes through communication between them to improve the position accuracy. Inter-distance measurement of nodes plays an important role in cooperative localization [11]–[15]. The inter-distance measurement includes the time of arrival (TOA) [16], time difference of arrival (TDOA), angle of arrival (AOA) [17], [18], and round trip time (RTT). RTT only required the time tag (i.e., the times of signal transmission, signal reception, and signal processing at both sides of the receivers), which is able to be easily implemented in VANET without any additional hardware overhead.

However, the non-line-of-sight (NLOS) delay may lead to the large inter-distance measurement error in an environment with more obstacles [19], [20]. In addition, the vehicles may suffer the malicious attacks [22]–[28] in VANET, such

The associate editor coordinating the review of this manuscript and approving it for publication was Maurice J. Khabbaz.

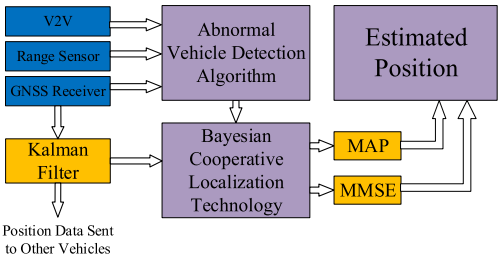

FIGURE 1. Scheme frame.

as V2V ranging manipulation [22], location spoofing [23], [26] and malicious message generation [24], which provides incorrect time tags to make ranging with neighboring vehicles erroneous and spreads distorted messages to the neighboring vehicles. The threat model are shown in detail:

NLOS link: The signal path between the vehicles is NLOS path, which results in an additional time delay for time tags. So the inter-distance measurement will be greater than real inter-distance.

Ranging manipulation: The vehicle A suffering from ranging manipulation provides delayed time-tags. The neighboring vehicle B of the A receives the incorrect time-tags, causing malicious error to inter-distance measurement.

Location spoofing: The vehicle A suffering from location spoofing will generate incorrect GNSS coordinates, resulting in its own positioning accuracy error. In addition, the location result of neighboring vehicle B will be affected if the B receives the mistaken coordinate of A.

Message distortion: The vehicle A suffering from Message distortion will transmits distorted message to its neighboring vehicle B. The B uses the distorted GNSS coordinate messages and distorted time-tag messages, which will damage the performance of cooperative localization.

To sum up, the performance of cooperative vehicle localization is seriously affected by NLOS link, inter-distance attacks and GNSS coordinates attacks. Therefore, the NLOS link and the malicious attack detection are required to ensure the credibility of localization before using the measured data to update the ego vehicle position. This paper constructs a new cooperative vehicle localization scheme in malicious vehicular network, and the framework is shown in Fig. 1. vehicle nodes in VANET obtain GNSS positioning information through the GNSS receiver, inter-distance information with neighboring vehicles through the range sensor, and exchange these measurements with each other through V2V. The main contributions of this paper are as follows:

1) The AVDA is proposed to detect malicious and NLOS vehicle in vehicular network. We analysis the statistic difference of LOS range measurement and abnormal range measurement. We also define the normalized detection variable with Mahalanobis Distance (MD), which is utilized to distinguish the normal vehicles from the abnormal vehicles.
2) The Bayesian cooperative localization method is proposed to find posterior probability of ego vehicle position. The method combines the GNSS measurement filtered by Kalman filter (KF) and range measurement selected by AVDA. We compare the performance of the method with two estimators, i.e., the posterior probability (MAP) estimator and minimum mean square error (MMSE) estimator.

This paper is organized as follows. Section II shows the related work. Section III defines the vehicular networks model and the range measurements model. In Section IV, we describe the proposed AVDA and Bayesian cooperative localization method in detail. In section V, we describe the simulation environment and verify the performance of the proposed scheme by using MATLAB and SUMO, and Section VI concludes the paper.

Sysmbol Notations: $\mathbf{A}$, $\mathbf{a}$, a, and $\mathcal{A}$ represent a matrix, a vector, a scalar, and a set, respectively; $\mathbf{A}^T$ denotes transpose of the matrix $\mathbf{A}$; $\|\mathbf{a}\|_0$ and $\|\mathbf{a}\|_2$ denote the length and the two-norm of vector $\mathbf{a}$; $\mathbb{E}\{a\}$ represents the expectation of a. $diag\{a_1, \ldots, a_n\}$ means a diagonal matrix whose main diagonal elements are $[a_1, \ldots, a_n]$. Tr$(\cdot)$ is the trace sum of matrix. Other specific symbols are explained as follows:

variables	Descriptions
$\mathbf{x}_e^*$	true state of ego vehicle
$\mathbf{x}_e^-$	predicted state of ego vehicle
$\mathbf{x}_e^f$	filtered state of ego vehicle
$\mathbf{x}_e^+$	estimated state of ego vehicle
$\mathbf{x}_n^-$	predicted state of n-th neighboring vehicle
$\mathbf{x}_n^f$	filtered state of n-th neighboring vehicle
$\mathbf{x}_n^+$	estimated state of n-th neighboring vehicle
$\mathbf{p}_e$	true position of ego vehicle
$\mathbf{p}_e^-$	predicted position of ego vehicle
$\mathbf{p}_e^f$	filtered position of ego vehicle
$\mathbf{p}_e^+$	estimated position of ego vehicle
$\mathbf{p}_n$	true position of ego vehicle
$\mathbf{p}_n^-$	predicted position of n-th neighboring vehicle
$\mathbf{p}_n^f$	filtered position of n-th neighboring vehicle
$\mathbf{p}_n^+$	estimated position of n-th neighboring vehicle
d_n	true range between ego vehicle and n-th neighboring vehicle
r_n	measured range between the ego vehicle and n-th neighboring vehicle

II. RELATED WORK

Recently, cooperative localization in VANET has attracted an increasing amount of attention. Ou in [13] proposed a roadside units (RSU)-based cooperative localization scheme in VANET. In the scheme, the vehicle retrieved the number

and positions of adjacent RSUs, then fixed the position of itself by measuring two-way TOAs. The author assumed that there was a pair of RSUs deployed on both sides of the road, communicating with the passing vehicles continuously. Thus, it required densely deployed RSUs on the road, the prohibitively high cost of RSU installation and the limitation in short time might kill the cooperative localization of VANET business case.

Cooperative localization approaches which benefited from mobile-to-mobile interactions (i.e., in terms of both measurements and exchanged location information) had been increasingly adopted [14], [15]. In [14], the authors used inter-vehicle distance measurements to improve the accuracy of vehicle location in GNSS-equipped VANETs. In their proposed localization framework, the inter-distance to neighboring vehicle was used to generate the location weight. The improved location was estimated by calculating a weighted sum over the locations. But the vehicles are restricted to single lane and do not communicate with vehicles in other lanes. Rohani *et al.* in [15] introduced data fusion to obtain high precision vehicle location. In their work, the inter-vehicle distance and GNSS location of neighboring vehicle were regarded as data source of data fusion technology. The method relieved the GNSS location error effectively. Whether as a weight factor or as a data source of data fusion, the accuracy of inter-vehicle distance was the basis of the accuracy of position estimation. However, these studies all assumed that vehicle measured the inter-vehicle distance in ideal vehicular network without NLOS link and malicious attacks.

The NLOS and malicious attack detections were necessary for cooperative localizations. NLOS detection have been investigated in some applications [20], [21]. A method to detect NLOS node based on the characteristics of autocorrelation matrix of distance measurement was proposed in [20]. Their proposed method could effectively detect NLOS node even without LOS node. But the detection performance was limited to the size of the distance value, it worked only at large distance. Li *et al.* [21] proposed a NLOS node location method based on firefly algorithm. According to the maximum likelihood method, the objective function was established by using the propagation probability of NLOS signal and LOS signal, and the NLOS node position was estimated by solving the objective function with firefly algorithm. To some extent, the method reduced the impact of NLOS error. However, it required the prior knowledge of NLOS error statistics, which was difficult to obtain in reality.

On a separate track, malicious attacks in the vehicular network have been studied [26]–[28]. In [26], a RSU with a uniform linear array (ULA) antenna measures the RSS and AOA of vehicle signals to estimate the actual distance and direction to the vehicle, which are then compared to the distance calculated using the vehicle's location coordinates. The method could eliminate the influence of location spoofing in vehicular network. However, the extra cost of the ULA antenna on the RSU made the business case difficult. In [27], the empirically determined thresholds were used to test whether the malicious vehicle was within the communication boundary, on the road, and obeying the speed limit. But they required the real-time estimation of communication boundary and the additional information (e.g., road map and speed limit). A malicious vehicle detection scheme utilizing the 1-hop table, where each vehicle cooperated with a reliable common reference vehicle to evaluate their neighboring vehicles was presented in [28]. The scheme required verified reliable vehicle in vehicular network, which was not satisfied in some real scenes. In addition, the authors given insufficient theoretical analysis.

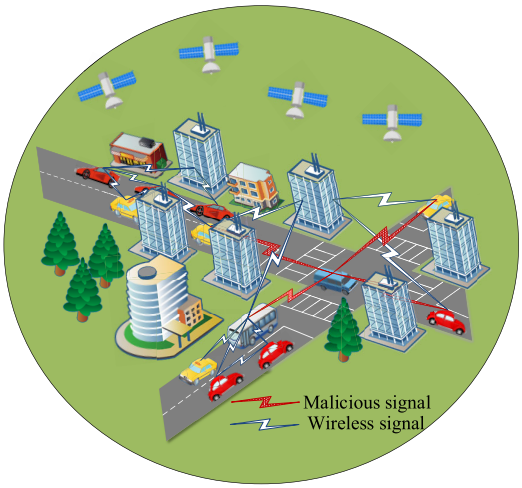

FIGURE 2. The vehicular network with NLOS path and malicious vehicle.

III. SYSTEM MODEL

A. VEHICULAR NETWORKS MODEL

Considering a network of N vehicles equipped with GNSS receiver and range sensor in two dimension space as exemplified in Fig. 2. Each vehicle (ego vehicle) connects to other vehicles (neighboring vehicles) among communicated range. There are NLOS measurements between vehicles due to the occlusion of obstacles to the wireless signal. And the malicious vehicle in the vehicular network spreads distorted information to its neighboring vehicles. $\mathcal{V}_N$ denotes the set of vehicles in the vehicular network. $\mathcal{V}_e$ is the set of N_e neighboring vehicle. Defining the abscissa as x-coordinate, the ordinate as y-coordinate in the two-dimensional space. $\mathbf{p}_i^{(k)} = [x_i^{(k)}\ y_i^{(k)}]$ and $\mathbf{v}_i^{(k)} = [v_i^{x(k)}\ v_i^{y(k)}]$ represent the position and velocity in x-coordinate and y-coordinate of the ego vehicle and n-th neighboring vehicle for $i = e$ and $i = n$ at time instant k respectively.

The state of the vehicle consists of its position and velocity. We define true state, predicted state, filtered state, and estimated state of vehicle.

a) The true state of the ego vehicle and neighboring vehicle can be found, respectively, as

$$\mathbf{x}_e^{*(k)} = \left[\mathbf{p}_e^{*(k)}, \mathbf{v}_e^{(k)}\right], \tag{1a}$$

$$\mathbf{x}_n^{*(k)} = \left[\mathbf{p}_n^{*(k)}, \mathbf{v}_n^{(k)}\right], \tag{1b}$$

where $\mathbf{p}_e^{*(k)}$ and $\mathbf{p}_n^{*(k)}$ are the true position of the ego vehicle and neighboring vehicle.

b) The predicted state of the ego vehicle and neighboring vehicle can be written, respectively, as

$$\mathbf{x}_e^{-(k)} = \left[\mathbf{p}_e^{-(k)}, \mathbf{v}_e^{(k)}\right], \tag{1c}$$

$$\mathbf{x}_n^{-(k)} = \left[\mathbf{p}_n^{-(k)}, \mathbf{v}_n^{(k)}\right], \tag{1d}$$

where $\mathbf{p}_e^{-(k)}$ and $\mathbf{p}_n^{-(k)}$ are the predicated position of the ego vehicle and neighboring vehicle, which are obtained by GNSS receiver.

c) The filtered state of the ego vehicle and neighboring vehicle can be expressed, respectively, as

$$\mathbf{x}_e^{f(k)} = \left[\mathbf{p}_e^{f(k)}, \mathbf{v}_e^{(k)}\right], \tag{1e}$$

$$\mathbf{x}_n^{f(k)} = \left[\mathbf{p}_n^{f(k)}, \mathbf{v}_n^{(k)}\right], \tag{1f}$$

where $\mathbf{p}_e^{f(k)}$ and $\mathbf{p}_n^{f(k)}$ are the filtered position of the ego vehicle and neighboring vehicle, which are obtained by Kalman filter described in subsection IV-A.

d) The estimated state of the ego vehicle and neighboring vehicle can be formulated, respectively, as

$$\mathbf{x}_e^{+(k)} = \left[\mathbf{p}_e^{+(k)}, \mathbf{v}_e^{(k)}\right], \tag{1g}$$

$$\mathbf{x}_n^{+(k)} = \left[\mathbf{p}_n^{+(k)}, \mathbf{v}_n^{(k)}\right], \tag{1h}$$

where $\mathbf{p}_e^{+(k)}$ and $\mathbf{p}_n^{+(k)}$ are the estimated position of the ego vehicle and neighboring vehicle, which are updated by the Bayesian cooperative localization method described in subsection IV-C.

B. RANGE MEASUREMENTS MODEL

The true range between the ego vehicle and the n-th neighboring vehicle is defined as

$$d_n^{(k)} = \left\|\mathbf{p}_n^{(k)} - \mathbf{p}_e^{(k)}\right\|_2. \tag{2}$$

The measured range from the ego vehicle to the neighboring vehicle is found as

$$r_n^{(k)} = d_n^{(k)} + m_n^{(k)} + nlos_n^{(k)} + \omega_n^{(k)}, \tag{3}$$

where $m_n^{(k)}$, $nlos_n^{(k)}$ and $\omega_n^{(k)}$ are the delay error of a malicious vehicle, NLOS delay error and range noise error, respectively. Further, different types of measured ranges are defined in the following:

a) Measured range with measurement error only can be written as

$$r_\omega^{(k)} = d_n^{(k)} + \omega_n^{(k)}, \tag{4a}$$

b) Measured range with NLOS delay can be formulated as

$$r_{nlos}^{(k)} = d_n^{(k)} + nlos_n^{(k)} + \omega_n^{(k)}, \tag{4b}$$

c) Measured range with malicious attack can be written as

$$r_m^{(k)} = d_n^{(k)} + m_n^{(k)} + \omega_n^{(k)}. \tag{4c}$$

The range measurement vector of N_e vehicles at k-th time instant as

$$\mathbf{r}^k = \mathbf{d}^{(k)} + \mathbf{n}^k + \mathbf{m}^k + \mathbf{w}^k, \tag{5}$$

where the n-th row of $\mathbf{r}^k$, $\mathbf{d}^{(k)}$, $\mathbf{n}^k$, $\mathbf{m}^k$, and $\mathbf{w}^k$ are $r_n^{(k)}$, $d_n^{*(k)}$, $nlos_n^{(k)}$, $m_n^{(k)}$, and $\omega_n^{(k)}$, respectively.

IV. BAYESIAN COOPERATIVE LOCALIZATION WITH ABNORMAL VEHICLE DETECTION

The proposed scheme aims to update vehicle position using normal vehicle measurement information selected by AVDA. We assume that each vehicle is able to obtain the position measurement and covariance matrix by GNSS receiver. We also suppose that each vehicle is able to obtain inter-vehicle distance measurements by range sensor.

A. GNSS WITH KF

There are errors in GNSS positioning results affected by measurement noise. Before cooperative positioning, KF algorithm is needed to preprocess GNSS localization results. We define the state of Kalman model as $\mathbf{s} = [p_x, v_x, a_x, p_y, v_y, a_y]$, the elements of which represent the vehicle position, velocity, and acceleration in x-coordinate and y-coordinate, respectively.

- *System state equation*:

$$\mathbf{s}_{(k|k)} = \mathbf{F}\mathbf{s}_{(k-1|k-1)} + \mathbf{b}_{(k-1)}, \tag{6}$$

where $\mathbf{F}$ is the state transition matrix obtained by acceleration model,i.e.

$$\mathbf{F} = \begin{bmatrix} \mathbf{A} & \mathbf{0} \\ \mathbf{0} & \mathbf{A} \end{bmatrix}, \quad \mathbf{A} = \begin{bmatrix} 1 & T & \frac{T^2}{2} \\ 0 & 1 & T \\ 0 & 0 & 1 \end{bmatrix}, \tag{7}$$

where T is the sample time; $\mathbf{b}$ is the process noise vector which describes the uncertainty of the state model. The noise is assumed to be additive zero-mean white Gaussian noise.

$$\begin{aligned} \mathbf{R}_{(k-1)} &= \mathbb{E}\{\mathbf{b}_{(k-1)}\mathbf{b}_{(k-1)}^T\} \\ &= diag\{\sigma_x^2, \sigma_{vx}^2, \sigma_{ax}^2, \sigma_y^2, \sigma_{vy}^2, \sigma_{ay}^2\}, \end{aligned} \tag{8}$$

where the elements on the diagonal in turn represent the error variance of each element variable in $\mathbf{s}_{(k)}$.

- *Measurement equation*:

$$\mathbf{z}_{(k|k)} = \mathbf{H}\mathbf{s}_{(k|k-1)} + \mathbf{c}, \tag{9}$$

where $\mathbf{H}$ is the measurement matrix and $\mathbf{c}$ is the measurement noise vector which describes the uncertainty of the measurement value. Here the measurement only consists of the position of vehicle from GNSS receiver. So we can obtain that

$$\mathbf{H} = \begin{bmatrix} 1 & 0 & 0 & 0 & 0 & 0 \\ 0 & 1 & 0 & 0 & 0 & 0 \end{bmatrix}, \tag{10}$$

$$\mathbf{Q} = \mathbb{E}\{\mathbf{v}\mathbf{v}^T\} = \begin{bmatrix} \hat{\sigma}^2_{\text{GNSS}} & 0 \\ 0 & \hat{\sigma}^2_{\text{GNSS}} \end{bmatrix}, \tag{11}$$

where $\hat{\sigma}^2_{GNSS}$ is the noise error variance of GNSS receiver.

After being preprocessed, the position information from GNSS is taken as the filtered data by KF in the following article, i.e, $\mathbf{p}_i^f = [p_x, p_y], i \in \{e, n\}$.

B. ABNORMAL VEHICLE DETECTION ALGORITHM

In this part, the purpose is to find the normal range measurements from all raw range measurements of ego vehicle. For explanation simplicity, the time index notation k is dropped.

According to [22], range measurement can be expressed by probability statistical model. The probability distribution of LOS measurement can be written as

$$Pr(r_n|\,\mathbf{p}_n, \mathbf{p}_e) = \frac{1}{\sqrt{2\pi\hat{\sigma}_n^2}} \exp\left[-\frac{1}{2\hat{\sigma}_n^2}\left(r_\omega^{(k)} - \left\|\mathbf{p}_n^- - \mathbf{p}_e^-\right\|_2\right)^2\right], \tag{12}$$

where $\hat{\sigma}_n^2 = \sigma_n^2 + \sigma_e^2 + \sigma_{r_n}^2$, $\sigma_n^2 = \text{Tr}\left(\mathbf{\Sigma}_n^{\mathbf{p}^-}\right)$, $\sigma_e^2 = \text{Tr}\left(\mathbf{\Sigma}_e^{\mathbf{p}^-}\right)$ are the sum of variances of normal measurement error, location uncertainty of the neighboring vehicle and the ego vehicle, respectively. $\mathbf{\Sigma}_e^{\mathbf{p}^-}$ and $\mathbf{\Sigma}_n^{\mathbf{p}^-}$ are the $[2\times2]$ position error covariance matrices of ego vehicle and its neighboring vehicle, respectively. Note that the GNSS receivers installed on ego vehicle and neighboring vehicle have the same performance and the vehicles are in similar environmental conditions. So $\mathbf{\Sigma}_e^{\mathbf{p}^-}$ and $\mathbf{\Sigma}_n^{\mathbf{p}^-}$ are considered to be the same, both equal to variance matrix of the GNSS receiver. w_n is measurement noise followed zero-mean Gaussian with variance $\sigma_{r_n}^2$.

The distribution of NLOS range measurement can be expressed as

$$Pr(r_n|\,nlos_n, \mathbf{p}_n, \mathbf{p}_e) = \frac{1}{\sqrt{2\pi\hat{\sigma}_n^2}} \exp\left[-\frac{1}{2\hat{\sigma}_n^2}\left(r_{nlos}^{(k)} - \left\|\mathbf{p}_n^- - \mathbf{p}_e^-\right\|_2\right)^2\right]. \tag{13}$$

Similarly, the distribution of malicious range measurement can be found as

$$Pr\,(r_n|\,m_n, \mathbf{p}_n, \mathbf{p}_e) = \frac{1}{\sqrt{2\pi\hat{\sigma}_n^2}} \exp\left[-\frac{1}{2\hat{\sigma}_n^2}\left(r_m^{(k)} - \left\|\mathbf{p}_n^- - \mathbf{p}_e^-\right\|_2\right)^2\right]. \tag{14}$$

From the distribution expression of NLOS range measurement and malicious range measurement, we obtain that the range measurements distribution disturbed by malicious attack are the same as those induced by NLOS delay, i.e., the Gaussian distribution with mean $\left\|\mathbf{p}_n^- - \mathbf{p}_e^-\right\|_2$ and variance σ_n^2. Our purpose is to get normal measurement. In addition, if the GNSS coordinates of ego or neighboring vehicle are attacked, the distribution should be expressed as

$$Pr(r_n|\,m_n, \mathbf{p}_n, \mathbf{p}_e) = \frac{1}{\sqrt{2\pi\hat{\sigma}_n^2}} \exp\left[-\frac{1}{2\hat{\sigma}_n^2}\left(r_\omega^{(k)} - \left\|\mathbf{p}_n^- + \mathbf{p}_m - \mathbf{p}_e^-\right\|_2\right)^2\right], \tag{15}$$

where GNSS coordinates error $\mathbf{p}_m$ is translated into malicious range error by 2-norm operation, so (14) reflects malicious attacks on GNSS coordinate and inter-distance. Therefore, the paper proposes the unified detection scheme to detect malicious attack and NLOS.

Due to the NLOS and malicious range are greater than LOS range, we obtain preliminarily LOS measurement from raw measurements using a simple threshold as

$$\begin{cases} n \in \mathcal{V}_1, & \text{if } \left|r_n - \left\|\mathbf{p}_n^- - \mathbf{p}_e^-\right\|_2\right| > \hat{\sigma}_n/2 \\ n \in \mathcal{V}_2, & \text{if } \left|r_n - \left\|\mathbf{p}_n^- - \mathbf{p}_e^-\right\|_2\right| \le \hat{\sigma}_n/2. \end{cases} \tag{16}$$

According to the decision result of (16), the range measurement vector $\mathbf{r}$ is reconstructed as

$$\mathbf{r} = \begin{bmatrix} \mathbf{r}_1 \\ \mathbf{r}_2 \end{bmatrix} \sim \mathcal{N}\left(\begin{bmatrix} \boldsymbol{\mu}_1 \\ \boldsymbol{\mu}_2 \end{bmatrix}, \begin{bmatrix} \mathbf{V}_{11} & \mathbf{V}_{12} \\ \mathbf{V}_{21} & \mathbf{V}_{22} \end{bmatrix}\right), \tag{17}$$

where $\mathbf{r}_1$ and $\mathbf{r}_2$ are range measurement vector corresponding to $\mathcal{V}_1$ and $\mathcal{V}_2$, $\boldsymbol{\mu}_1$ and $\boldsymbol{\mu}_2$ are mean vector of $\mathbf{r}_1$ and $\mathbf{r}_2$, $\mathbf{V}_{11}$, $\mathbf{V}_{12}$, $\mathbf{V}_{21}$, and $\mathbf{V}_{22}$ are covariance matrices of size $\left[\|\mathbf{r}_1\|_0 \times \|\mathbf{r}_1\|_0\right]$, $\left[\|\mathbf{r}_1\|_0 \times \|\mathbf{r}_2\|_0\right]$, $\left[\|\mathbf{r}_2\|_0 \times \|\mathbf{r}_1\|_0\right]$ and $\left[\|\mathbf{r}_2\|_0 \times \|\mathbf{r}_2\|_0\right]$, respectively.

The decision algorithm (16) has a conservative rule that accepts only the measurements having less than half of sigma (i.e., $\hat{\sigma}_n$) error from the expected value for LOS. So $\mathcal{V}_1$ may contain some LOS elements. In order to obtain as many normal measurements as possible, we need to further detect the range measurements.

When $\mathbf{r}_1$ is LOS range measurement, conditional variable $\mathbf{r}_1|\mathbf{r}_2$ has a central χ^2 distribution with $\|\mathbf{r}_1\|_0$ degrees of freedom (DOF). To test whether the measurements in $\mathbf{r}_1$ are corrupted by NLOS delay, the Mahalanobis Distance (MD) is introduced. We define normalized detection variable as the square of MD [29], i.e.,

$$Z_{\mathbf{r}_1} = \left(\mathbf{r}_1 - \boldsymbol{\mu}_{1|2}\right)^T \mathbf{V}_{1|2}^{-1}\left(\mathbf{r}_1 - \boldsymbol{\mu}_{1|2}\right), \tag{18}$$

where

$$\boldsymbol{\mu}_{1|2} = \boldsymbol{\mu}_1 + \mathbf{V}_{12}\mathbf{V}_{22}^{-1}\left(\mathbf{r}_2 - \boldsymbol{\mu}_2\right), \tag{18a}$$

$$\mathbf{V}_{1|2} = \mathbf{V}_{11} - \mathbf{V}_{12}\mathbf{V}_{22}^{-1}\mathbf{V}_{21}. \tag{18b}$$

Note that the value of $Z_{\mathbf{r}_1}$ is the sum of the MD squares of all measurements in $\mathbf{r}_1$. To test each measurement in $\mathbf{r}_1$ individually, there are $\|\mathbf{r}_1\|_0$ times 1 DOF χ^2-tests to be performed. Define the credibility of a single vehicle as

$$q_1^i = 1 - \int_0^{Z_i} f_{\chi_1^2}(t)dt, \tag{19}$$

where Z_i is the MD square corresponding to i-th element of $\mathbf{r}_1$. Due to the elements of the $\mathbf{r}_2$ are considered as LOS measurements, we set the credibility of those $q_2^i = 1$. Now we have the credibility of all measurements. Then we reallocate the elements of $\mathbf{r}$ in two group using their credibility, i.e.,

$$\begin{cases} n \in \hat{\mathcal{V}}_1, & \text{if } q_j^i < \gamma \\ n \in \hat{\mathcal{V}}_2, & \text{if } q_j^i \ge \gamma \end{cases} \tag{20}$$

Algorithm 1 Abnormal Vehicle Detection Algorithm

Require: GNSS location of ego vehicle $\mathbf{p}_e^{-(k)}$, GNSS location of neighboring vehicle $\mathbf{p}_n^{-(k)}$, inter-distance measurements $r_n^{(k)}$

Ensure: Normal vehicle set $\hat{\mathcal{V}}_2$, normal inter-distance measurements $r_m^{(k)}$

for $k = 1$ to K time index **do**
  $\forall e \in \mathcal{V}_N$:
  Initialize self location by GNSS receiver, $\mathbf{p}_e^{-(k)}$
  Receive neighboring vehicle GNSS location, $\mathbf{p}_n^{-(k)}$
  Receive inter-distance measurements, $r_n^{(k)}$
  for $e = 1$ to N in parallel **do**
    if $\left| r_n^k - \left\| \mathbf{p}_n^{-(k)} - \mathbf{p}_e^{-(k)} \right\|_2 \right| > \hat{\sigma}_n/2$ **then**
      $\mathcal{V}_1 \leftarrow n, \mathbf{r}_1 \leftarrow r_n^{(k)}$
    else
      $\mathcal{V}_2 \leftarrow n\,, \mathbf{r}_2 \leftarrow r_n^{(k)}$
    end if
    for $i = 1$ to length $(\mathbf{r}_1)$ **do**
      Compute the normalized detection variable $Z_{\mathbf{r}_i}$ (18)
      Compute credibility q_1^i (19)
    end for
    Set the credibility of the elements of $\mathbf{r}_2$ are 1, i.e. $q_2^i = 1$
    Get normal vehicle by all credibility $\hat{\mathcal{V}}_2$ (20)
    Get normal range measurements $r_m^{(k)}, m \in \hat{S}_2$
  end for
end for

where $j \in \{1, 2\}$ and γ is threshold. The proposed AVDA is summarized in Algorithm 1, and includes the following three steps:

Step 1: We divide all neighboring vehicles into two group through a conservative threshold, a group of vehicles that are temporarily considered abnormal $\mathcal{V}_1$ and a group of normal vehicles $\mathcal{V}_2$. The corresponding range measurement vectors are $\mathbf{r}_1$ and $\mathbf{r}_2$, respectively.

Step 2: We obtain the normalized detection variable $Z_{\mathbf{r}_1}$ by the MD between $\mathbf{r}_1$ and $\mathbf{r}_2$. Using $Z_{\mathbf{r}_1}$ to calculate the credibility of neighboring vehicles in $\mathcal{V}_1$.

Step 3: We obtain the group of normal vehicles $\hat{\mathcal{V}}_2$ and normal range measurement vector $\hat{\mathbf{r}}_2$ by the credibility of neighboring vehicles.

C. UPDATE EGO VEHICLE POSITION WITH BAYESIAN COOPERATIVE LOCALIZATION METHOD

In subsection IV-B, we use the statistical method to detect abnormal vehicle caused by NLOS delay and malicious attack. Now the $\hat{\mathcal{V}}_2$ will be fully utilized to improve the positioning accuracy of ego vehicle with the help of a Bayesian cooperative positioning method [15].

In the vehicle network, ego vehicle receives the observations from its neighboring vehicles. The observations can be expressed as

$$\mathbf{p}_e^n = \mathbf{p}_n + r_n \begin{bmatrix} \cos\theta_n \\ \sin\theta_n \end{bmatrix}, \tag{21}$$

where θ_n is the bearing of the inter-vehicle distance measurement. But this paper assumes that the range sensor only provides inter-vehicle distance measurement, not the bearing.

First, we consider that there is a single normal vehicle near the ego vehicle. According to Bayesian theory, we establish as

$$f_{\mathrm{p}_e|\mathrm{p}_e^1}\left(\mathbf{p}_e \middle| \mathbf{p}_e^1\right) = \frac{f_{\mathrm{p}_e^1|\mathrm{p}_e}\left(\mathbf{p}_e^1 \middle| \mathbf{p}_e\right) \cdot f_{\mathrm{p}_e}(\mathbf{p}_e)}{f_{\mathrm{p}_e^1}\left(\mathbf{p}_e^1\right)}. \tag{22}$$

The left of (22) is post-probability density of ego vehicle position observed at given a neighboring vehicle observation, $f_{\mathrm{p}_e^1|\mathrm{p}_e}\left(\mathbf{p}_e^1 \middle| \mathbf{p}_e\right)$ is likelihood function. $f_{\mathrm{p}_e}(\mathbf{p}_e)$ and $f_{\mathrm{p}_e^1}\left(\mathbf{p}_e^1\right)$ are PDFs of the ego vehicle's position and neighboring vehicle observation. The latter one can be obtained by independence between range measurement and position measurement. Using the model (21), we found

$$F_{\mathrm{p}_e^1}\left(\mathbf{p}_e^1\right) = \int_{-\infty}^{+\infty} \int_{-\infty}^{\mathbf{p}_1 - \mathbf{p}_e^1} f_{\mathrm{p}_1 \mathrm{d}_1}(\mathbf{p}_1, d_1) d\mathbf{p}_1 d d_1. \tag{23}$$

Differentiating with respect to d_1 in (23), the PDF can be derived as

$$f_{\mathrm{p}_e^1}\left(\mathbf{p}_e^1\right) = \int_{-\infty}^{+\infty} f_{\mathrm{p}_1 \mathrm{d}_1}\left(\mathbf{p}_1, \mathbf{p}_1 - \mathbf{p}_e^1\right) d\mathbf{p}_1. \tag{24}$$

Since vehicle position and range come from different sensor, the joint probability distribution of $\mathbf{p}_1$ and d_1 can be expressed by the product of the corresponding probability distributions. So (24) can be written as

$$f_{\mathrm{p}_e^1}\left(\mathbf{p}_e^1\right) = \int_{-\infty}^{+\infty} f_{\mathrm{p}_1}(\mathbf{p}_1) \cdot f_{\mathrm{d}_1}\left(\mathbf{p}_1 - \mathbf{p}_e^1\right) d\mathbf{p}_1. \tag{25}$$

Similarly, we obtain likelihood function as

$$f_{\mathrm{p}_e^1|p_e}\left(\mathbf{p}_e^1 | \mathbf{p}_e\right) = \int_{-\infty}^{+\infty} f_{\mathrm{p}_1}(\mathbf{p}_1 | \mathbf{p}_e) \cdot f_{\mathrm{d}_1}\left(\mathbf{p}_1 - \mathbf{p}_e^1 | \mathbf{p}_e\right) d\mathbf{p}_1. \tag{26}$$

Ego vehicle and its neighboring vehicles are supposed to be sufficient far apart to ensure independence of their position measurement. Thus, (25) and (26) can be developed to

$$\begin{aligned} f_{\mathrm{p}_e^1}\left(\mathbf{p}_e^1\right) &= \int_{-\infty}^{+\infty} f_{\mathrm{p}_e}(\mathbf{p}_e) \cdot f_{\mathrm{p}_e^1|\mathrm{p}_e}\left(\mathbf{p}_e^1 | \mathbf{p}_e\right) d\mathbf{p}_e \\ &= \int_{-\infty}^{+\infty} \int_{-\infty}^{+\infty} f_{\mathrm{p}_e}(\mathbf{p}_e) \cdot f_{\mathrm{p}_1}(\mathbf{p}_1) \\ &\quad \cdot f_{\mathrm{d}_1}(\mathbf{p}_1 - \mathbf{p}_e) d\mathbf{p}_1 d\mathbf{p}_e, \end{aligned} \tag{27}$$

$$f_{\mathrm{p}_e^1|\mathrm{p}_e}\left(\mathbf{p}_e^1 \middle| \mathbf{p}_e\right) = \int_{-\infty}^{+\infty} f_{\mathrm{p}_1}(\mathbf{p}_1) \cdot f_{\mathrm{d}_1}(\mathbf{p}_1 - \mathbf{p}_e) d\mathbf{p}_1. \tag{28}$$

Substituting (27) and (28) into (22), (22) can expressed in (29), as shown at the bottom of next page.

Now we extend it to the multi-neighboring vehicles scenario. We approximate the prior PDF of vehicle position and

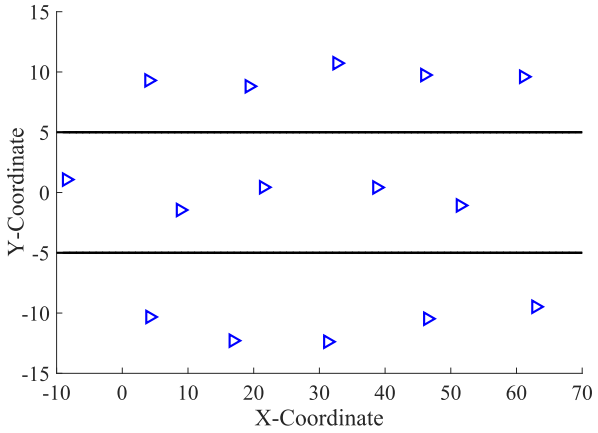

FIGURE 3. The initial position of vehicle.

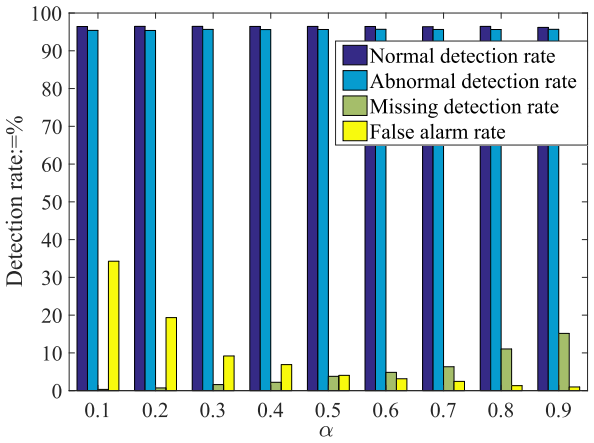

FIGURE 4. The detection rates of AVDA under different α.

range by the filtered vehicle position and range measurement respectively, i.e.,

$$\mathbf{p}_i \sim \mathcal{N}\left(\mathbf{p}_i^f, \sigma_i^2\right) = f_{\mathrm{p}_i^f}\left(\mathbf{p}_i\right), \quad i \in (e, m), \tag{30}$$

$$d_m \sim \mathcal{N}\left(r_m, \sigma_r^2\right) = f_{\mathrm{d}_m}\left(r_m\right), \tag{31}$$

where $\mathbf{p}_i^f$ is position data filtered by the Kalman filter described in subsection IV-A, r_m is measured inter-vehicle distance data, and σ_r^2 is variance of range sensor.

Similar to (29), we get the post PDF of ego vehicle position in the case of N_2 neighboring vehicles. Therefore, in multi-neighboring vehicles case, (29) can be derived as (32), as shown at the bottom of this page.

Finally the estimated position of ego vehicle is obtained by MAP or MMSE as

$$\mathbf{p}_{map}^{+} = \arg\max_{\mathbf{p}_e} f_{\mathrm{p}_e|\mathrm{p}_e^1,\ldots,\mathrm{p}_e^{N_2}}\left(\mathbf{p}_e|\mathbf{p}_e^1,\ldots,\mathbf{p}_e^{N_2}\right), \tag{33}$$

$$\mathbf{p}_{mmse}^{+} = \int_{-\infty}^{+\infty} \mathbf{p}_e f_{\mathrm{p}_e|\mathrm{p}_e^1,\ldots,\mathrm{p}_e^{N_2}}\left(\mathbf{p}_e|\mathbf{p}_e^1,\ldots,\mathbf{p}_e^{N_2}\right) d\mathbf{p}_e. \tag{34}$$

D. PROCESS OF WHOLE PROPOSED SCHEME

In the section, we describe the process of whole proposed cooperative vehicle localization scheme. Specifically, each ego vehicle obtains its GNSS location and collects the GNSS locations of neighbors and the inter-distance measurement at k-th moment. These GNSS locations are pre-processed by KF. To provide the normal inter-distance measurement for cooperative localization, the AVDA is applied, which is detailed in Algorithm 1. In the algorithm, firstly ego vehicle obtains partial normal inter-distance measurements $\mathbf{r}_2$ from all raw measurements by a conservative threshold. The rest of raw measurements are treated as abnormal $\mathbf{r}_1$ temporarily, which needs to be further detected . Then the detection variables Z_{r_i} of inter-distance measurements of $\mathbf{r}_1$ are calculated to further get the credibility q_1^i of the corresponding neighboring vehicles. Finally, the detection based on the credibility is implemented to obtain all normal inter-distance measurements $r_m^{(k)}$ and normal neighboring vehicles $\hat{\mathcal{V}}_2$.

Based on $\hat{\mathcal{V}}_2$ and $r_m^{(k)}$ obtained by AVDA, the Bayesian cooperative localization method is applied to estimate the ego vehicle location. In the method, the pre-processed GNSS locations $\mathbf{p}_i^f$ $(i \in \{e, \hat{\mathcal{V}}_2\})$ and normal inter-distance measurements $r_m^{(k)}$ are regarded as mean value to approximate the vehicle location prior-PDFs and the inter-distance prior-PDFs. Based these location prior-PDFs, ego vehicle generates N_p ego location particles and N_p neighbor location particles. According to the idea of Monte Carlo method, these location particles are substituted into the (32), and the posterior probabilities of N_p ego location particles are calculated with $N_p * N_p$ cycles. Based on these posterior probabilities, the final location of ego vehicle is estimated using MAP and MMSE.

$$f_{\mathrm{p}_e|\mathrm{p}_e^1}\left(\mathbf{p}_e|\mathbf{p}_e^1\right) = \frac{\int_{-\infty}^{+\infty} f_{\mathrm{p}_1}\left(\mathbf{p}_1\right)\cdot f_{\mathrm{d}_1}\left(\mathbf{p}_1-\mathbf{p}_e\right)d\mathbf{p}_1\cdot f_{\mathrm{p}_e}\left(\mathbf{p}_e\right)}{\int_{-\infty}^{+\infty}\int_{-\infty}^{+\infty} f_{\mathrm{p}_e}\left(\mathbf{p}_e\right)\cdot f_{\mathrm{p}_1}\left(\mathbf{p}_1\right)\cdot f_{\mathrm{d}_1}\left(\mathbf{p}_1-\mathbf{p}_e\right)d\mathbf{p}_1 d\mathbf{p}_e} \tag{29}$$

$$f_{\mathrm{p}_e|\mathrm{p}_e^1,\mathrm{p}_e^2,\ldots,\mathrm{p}_e^{N_2}}\left(\mathbf{p}_e|\,\mathbf{p}_e^1,\mathbf{p}_e^2,\ldots,\mathbf{p}_e^{N_2}\right) = \frac{\prod_m^{N_2}\int_{-\infty}^{+\infty} f_{\mathrm{p}_m^f}\left(\mathbf{p}_m\right)\cdot f_{\mathrm{d}_m}\left(\mathbf{p}_m-\mathbf{p}_e\right)d\mathbf{p}_m\cdot f_{\mathrm{p}_e^f}\left(\mathbf{p}_e\right)}{\prod_m^{N_2}\int_{-\infty}^{+\infty}\int_{-\infty}^{+\infty} f_{\mathrm{p}_e^f}\left(\mathbf{p}_e\right)\cdot f_{\mathrm{p}_m^f}\left(\mathbf{p}_m\right)\cdot f_{\mathrm{d}_m}\left(\mathbf{p}_m-\mathbf{p}_e\right)d\mathbf{p}_m d\mathbf{p}_e} \tag{32}$$

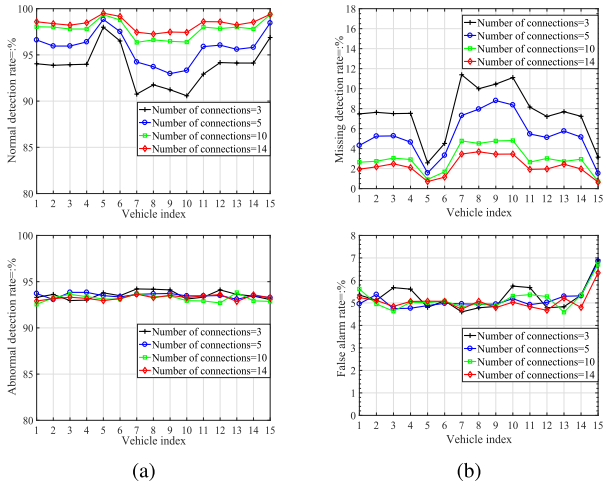

FIGURE 5. The normal detection rates, abnormal detection rates,missing detection rate, and false alarm rate of the 15 vehicles in the four scenarios.

V. PERFORMANCE EVALUATION

A. SIMULATION SCENARIO AND ENVIRONMENT

In vehicular network, 15 vehicles spread in the 3 lanes, with 5 vehicles in each lane. It is assumed that the vehicle nodes in network can realize instant communication to exchange GNSS measurements and inter-distance measurements. The ground true position of each vehicle at initial time can be expressed as

$$\mathbf{p}_b^{(1)} = \mathbf{p}_1^{(1)} + \begin{bmatrix} 15, & 0 \\ 15, & 0 \\ 15, & 0 \end{bmatrix} + \Theta_b, \quad b \in (2,3,4,5)\,, \quad (35)$$

where

$$\mathbf{p}_1^{(1)} = \begin{bmatrix} -10, & 10 \\ -20, & 0 \\ -10, & -10 \end{bmatrix}, \quad (36)$$

Θ_b is random matrix whose elements follow uniform distribution $\mathcal{U}(-2, 2)$ for varying formation of the vehicular network in simulation. Fig. 3 draws the initial locations of all vehicles and the initial vehicular network topology. At each time slot, the ego vehicle and the neighboring vehicles are considered as relatively static.

In the simulation scenario, all vehicles move along the road at same direction. Ego vehicle moves at initial stable velocity $\mathbf{v}^{(1)}$=[25, 0], then change its velocity at uniform acceleration successively until $\mathbf{v}^{(k)} = [-25, 0]$. Define the ratio α as the ratio of the number of abnormal vehicles to the number of neighboring vehicles. We select some vehicles as attacked vehicles and NLOS vehicles in vehicular network by the ratio α. The simulation parameters are shown in Table 1.

B. PERFORMANCE ANALYSIS

In this subsection, we investigate the performance of the proposed scheme in MATLAB software. The proposed AVDA and Bayesian cooperative localization method are executed

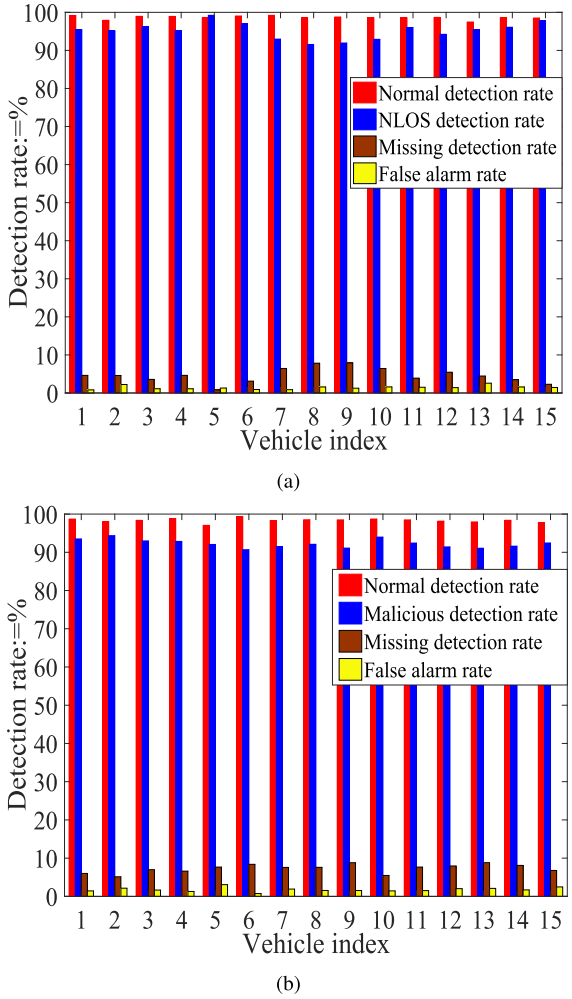

FIGURE 6. The detection performance of AVDA against NLOS (a) and malicious attacks (b).

TABLE 1. Simulation Parameters.

Parameter	value	Parameter	Value
T	1 (sec)	γ	0.8
σ_{r_n}	2 (m)	σ_{GNSS}	3.0 (m)
σ_n	$\hat{\sigma}_{\text{GNSS}}$	σ_e	$\hat{\sigma}_{\text{GNSS}}$
σ_x	0.01 (m)	σ_y	0.01 (m)
σ_{vx}	0.01 $(m\cdot s^{-1})$	σ_{vy}	0.01 $(m\cdot s^{-1})$
σ_{ax}	0.01 $(m\cdot s^{-2})$	σ_{ay}	0.01 $(m\cdot s^{-2})$

180 times continuously in a experiment. We repeat the experiment 10 times, taking the average value as the result.

We first focus on the performance of AVDA. The malicious inter-distance error and the NLOS bias are generated from uniform distribution $m_n^k \sim \mathcal{U}(5, 20)$ and $nlos_n^k \sim \mathcal{U}(0.5d_n^{(k)}, 0.75d_n^{(k)})$, respectively. Fig. 4 describes the detection rates of AVDA under different α. With the increase of α, the missing detection rate decreases and the false alarm rate increases. When α is 0.5, AVDA shows the optimal detection performance. Considering four scenarios: the number of connections to the ego vehicle are 3, 5,

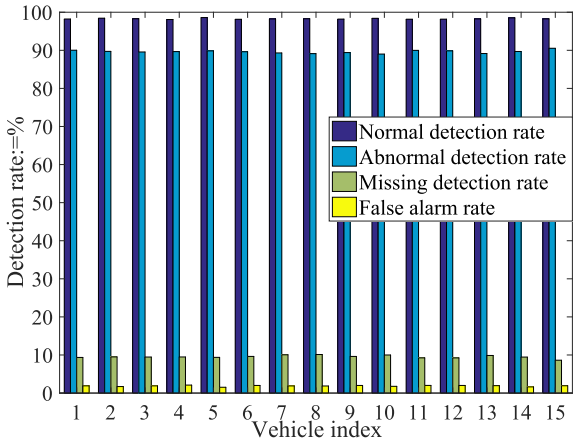

FIGURE 7. The detection rate when abnormal inter-distance measurement error close to GNSS measurement error.

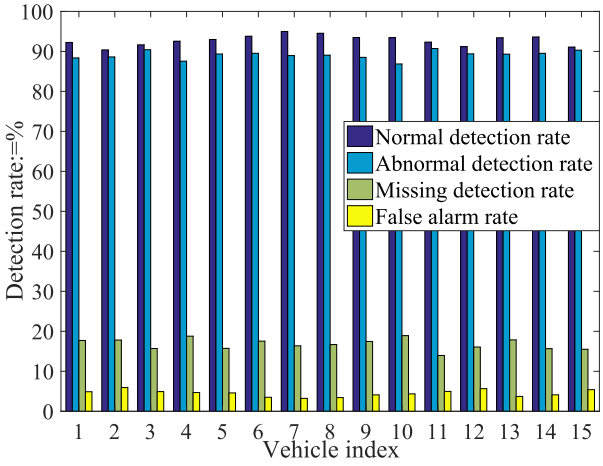

FIGURE 8. The detection rates of AVDA when both the ranging measurement and the GNSS measurements are under the malicious attacks.

10 and 14, respectively. We perform 180 times the algorithm and compute the averages in the four scenarios, respectively. Fig. 5 shows the normal detection rate, missing detection rate, abnormal detection rate, and false alarm rate of AVDA with different number of connections. As shown in Fig. 5-(a), the normal detection rates and abnormal detection rates of the 15 vehicles in the four scenarios are more than 90% when the credibility threshold γ=0.8. Meanwhile, Fig. 5-(b) shows the missing detection rates are less than 7% and false alarm rates are less than 12%.

Then, we consider all connectivity network, i.e., the number of connections allowed for each vehicle equals to 14. We study the detection performance of AVDA against malicious attacks and NLOS respectively. As shown in the Fig. 6, AVDA also achieves excellent performance for the detection of these two kinds of abnormal measurement. The malicious detection rate and NLOS detection rate are both above 90%. The missing detection rates and false alarm rates remain low probability. Fig. 7 shows the detection performace of AVDA

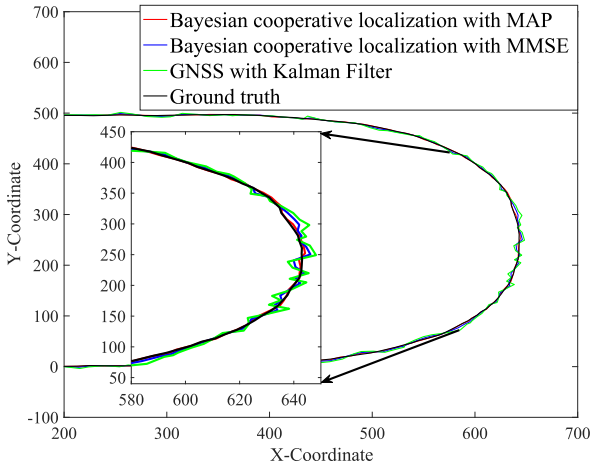

FIGURE 9. The partial path of a special ego vehicle with ground truth location, filtered predicted location, and estimated location with MAP and MMSE.

under the condition that the abnormal inter-distance measurement error is close to GNSS error. Abnormal inter-distance measurement error is set to 5 m, close to $\sqrt{2}\sigma_{GNSS}$. Compared with the condition that abnormal inter-distance error larger than GNSS measured error, the performances of AVDA are still good. The normal detection rate and abnormal detection rate are kept above 90%, while the missing detection rate and false alarm rate are lower 10%. Note that AVDA must satisfy the condition that there is LOS vehicle near the ego vehicle. If all the inter-vehicle distances between the ego vehicle and the neighboring vehicles are measured from NLOS and malicious attack, the AVDA may not work.

The malicious GNSS x and y coordinate error are generated from uniform distribution $\mathcal{U}(10, 20)$. Fig. 8 shows the detection rates of AVDA when both the ranging measurement and the GNSS measurements are under the malicious attacks. The results show that the normal detection rate and abnormal detection rate are approximate 90%. But the missing detection rate indicates that the more abnormal vehicles are decided to normal vehicles. To sum up, the proposed AVDA has excellent detection performance for NLOS link, inter-distance attacks and GNSS coordinate attacks, especially for the former two.

Finally, we compare the four different localization methods: GNSS, GNSS with Kalman filter, Bayesian cooperative localization with MMSE, and Bayesian cooperative localization with MAP. GNSS means stand-alone GNSS positioning method. GNSS with Kalman filter is to use Kalman filter to filter the GNSS positioning results to improve the GNSS positioning accuracy. The last two methods are the proposed localization with two different estimators, i.e. MAP and MMSE. Fig. 9 shows partial path of a special ego vehicle with ground truth position, filtered position and estimated position. Fig. 9 illustrates the trajectories estimated by the proposed scheme and ground truth are basically the same,

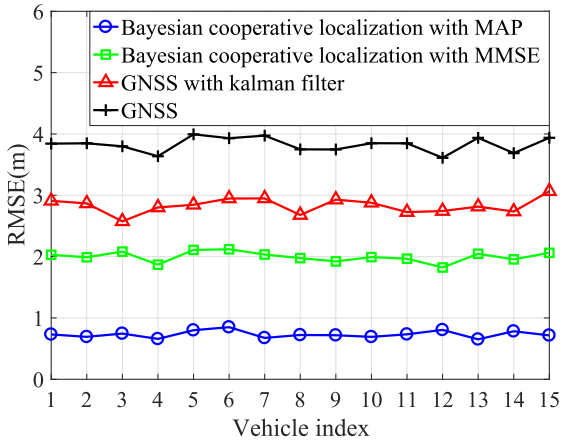

FIGURE 10. The localization error of bayesian cooperative localization with MAP and MMSE, and GNSS with Kalman Filter, and GNSS.

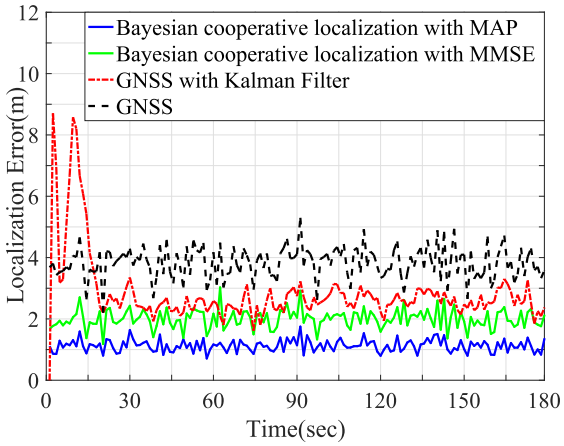

FIGURE 11. The RMSE of bayesian cooperative localization with MAP and MMSE, and GNSS with Kalman Filter, and GNSS.

which indicates the proposed scheme achieves good effect in location tracing.

Fig. 10 and Fig. 11 compare the localization precision of different positioning methods. As shown in the two figures, the proposed scheme improves the positioning accuracy effectively within the malicious and NLOS vehicular network. Fig. 11 shows that the RMSE of the proposed localization scheme is optimized to approximate 2 meters with MMSE and sub-meter with MAP.

C. REAL SCENARIO WITH SUMO-SIMULATED TRAFFIC

To verify the scheme performance in a more realistic environment, we use the traffic simulator SUMO, which uses real city maps to generate synthetic traces of vehicles. For this experiment, we consider a special vehicle (ego vehicle) constrained to the highlighted streets in Fig. 11, in three areas of Beijing (China). Ego vehicle receives the information from the neighboring vehicles when driving on the streets. In particular, we generate 300, 600, 500 vehicles to pass through these areas in 1000 seconds, respectively. We assume that each vehicle is equipped with a GNSS receiver to obtain itself GNSS position. Since GNSS positioning performance is sensitive to surround environment, we model three types of conditions which affect the GNSS positioning accuracy differently, as shown in Table 2. In vehicular network, the generation of NLOS vehicle and malicious vehicle refers to subsection IV-A. In vehicular network, we randomly select two neighbor vehicles as the malicious vehicles and half of the connected vehicles as the NLOS vehicles at each time slot. The malicious error and the NLOS bias are generated from uniform distribution $m_n^k \sim \mathcal{U}(10, 20)$ and $nlos_n^k \sim \mathcal{U}(0.5d_n^{(k)}, 0.75d_n^{(k)})$, respectively. We repeat the experiment 10 times, taking the average as the final result.

TABLE 2. The GNSS uncertainty of three types of conditions.

Condition	Environment	GNSS uncertainty
C-I	Open sky rural, large road with 3 × 3 lane, scattered med-size buildings.	Nominal $\hat{\sigma}_{\text{GNSS}} = \sigma_{\text{GNSS}}$
C-II	Some obstacles urban and narrow road with 2×2 lane, scattered medium size buildings.	Slightly degraded $\hat{\sigma}_{\text{GNSS}} = 2\sigma_{\text{GNSS}}$
C-III	Ultra narrow road with 2 lane, scattered large size buildings.	Severely degraded $\hat{\sigma}_{\text{GNSS}} = 4\sigma_{\text{GNSS}}$

In Fig. 12, the top three sub-figures show real time satellite images of the three conditions listed in Table 2, and the highlighted part are roads through which the vehicles pass; the bottom three sub-figures describe the cumulative distribution functions (CDFs) of the vehicle location error under the three conditions listed in Table 2, for Bayesian cooperative localization with MMSE (blue line) and Bayesian cooperative localization with MAP (red line) and stand-alone GNSS (orange line). Figs. 12-(a), (b) and (c) show that in the environments that scatter different size buildings, the proposed scheme improves the localization result of GNSS effectively, and the localization performances using MAP is similar with those using MMSE.

Fig. 13 shows that the detection performance of AVDA when the number of connection is time-varying. The AVDA remains superior detection performance. The abnormal detection rate and normal detection rate are maintained 90% approximately, and the missing detection rate and false alarm rate are lower than 10%.

D. COMPUTATIONAL COMPLEXITY

Ego vehicle needs to communicate to N_e neighboring vehicle, which induces a computational cost of $O(N_e)$. AVDA performs NLOS and malicious detection on N_e neighboring vehicles, resulting in a computational complexity of $O(N_e)$. The proposed Bayesian cooperative localization method needs to integrate the measurement of N_e neighboring vehicles, and this method is realized by Monte Carlo simulation with particle number N_p, so its computational complexity is $O(N_p * N_e)$.

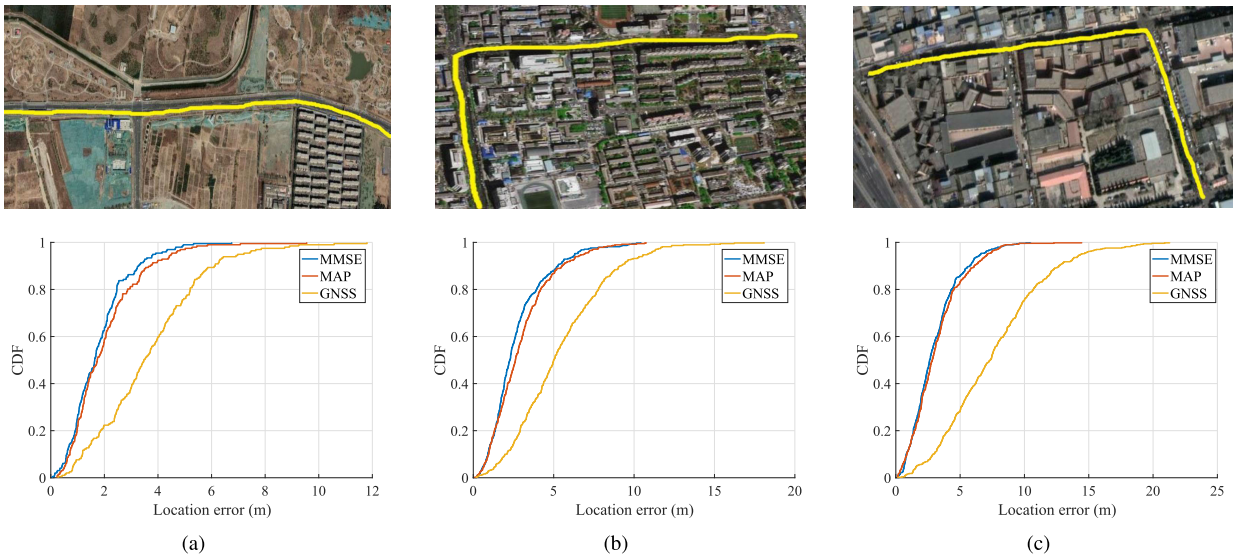

FIGURE 12. The turely traces (top) and CDFs (buttom) of the vehicle location error for the C-I (a), C-II (b), C-III (c) in Table 2, for the bayesian cooperative localization with MMSE and the bayesian cooperative localization with MAP and stand-alone GNSS.

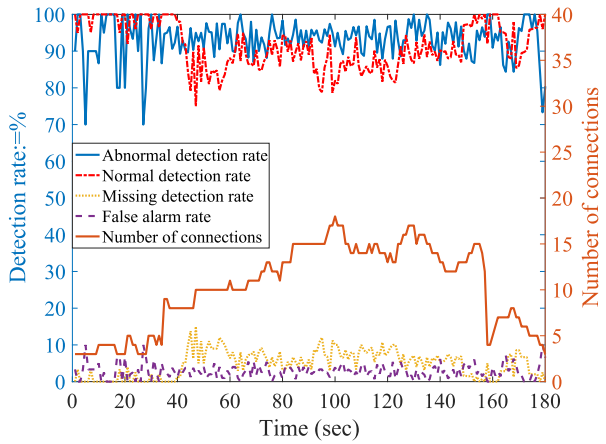

FIGURE 13. The detection rate of AVDA when the number of connections is time-varying.

Therefore, the computational complexity of each ego vehicle is $O((N_p + 2) * N_e)$, the overall complexity is $O((N_p + 2) * N_e) * N)$ in network of N vehicles.

VI. CONCLUSION

This paper has proposed an AVDA method to detect the NLOS vehicles and the malicious vehicles by using the range measurements and predicted position in VANET. The method firstly gets the probability normal neighboring vehicles through a conservative threshold; then obtaining the credibility of all neighboring vehicles by performing several times 1 DOF χ^2 test. The proposed Bayesian cooperative localization method with AVDA has been implemented into the cooperative localization scheme with MAP and MMSE estimator, which effectively improves the position accuracy by combining selected range and position measurements. The simulated results demonstrate the proposed scheme could improve the vehicle localization accuracy in NLOS and malicious vehicle environment compared to stand-alone GNSS solution. Moreover, the localization scheme was validated in real urban scenarios using the SUMO traffic simulator.

REFERENCES

[1] J. Zhang, F.-Y. Wang, K. Wang, W.-H. Lin, X. Xu, and C. Chen, "Data-driven intelligent transportation systems: A survey," *IEEE Trans. Intell. Transp. Syst.*, vol. 12, no. 4, pp. 1624–1639, Dec. 2011.

[2] L. C. Bento, P. Bonnifait, and U. J. Nunes, "Set-membership position estimation with GNSS pseudorange error mitigation using lane-boundary measurements," *IEEE Trans. Intell. Transp. Syst.*, vol. 20, no. 1, pp. 185–194, Jan. 2019.

[3] E. Kaplan and C. Hegarty, *Understanding GPS: Principles and Applications*. Norwood, MA, USA: Artech House, 2006.

[4] M. Skoglund, T. Petig, B. Vedder, H. Eriksson, and E. M. Schiller, "Static and dynamic performance evaluation of low-cost RTK GPS receivers," in *Proc. IEEE Intell. Vehicles Symp. (IV)*, Jun. 2016, pp. 16–19.

[5] T. Yu, J. Zhao, and Y. Gong, "UAV-aided localization algorithm with relay for train-mounted mobile terminals," *Phys. Commun.*, vol. 34, pp. 227–234, Jun. 2019.

[6] H. Wymeersch, J. Lien, and M. Z. Win, "Cooperative localization in wireless networks," *Proc. IEEE*, vol. 97, no. 2, pp. 427–450, Feb. 2009.

[7] J. Zhao, S. Ni, L. Yang, Z. Zhang, Y. Gong, and X. You, "Multiband cooperation for 5G HetNets: A promising network paradigm," *IEEE Veh. Technol. Mag.*, vol. 14, no. 4, pp. 85–93, Dec. 2019.

[8] J. Xu, P. Zhu, J. Li, X. Wang, and X. You, "Secrecy energy efficiency optimization for multi-user distributed massive MIMO systems," *IEEE Trans. Commun.*, vol. 68, no. 2, pp. 915–929, Feb. 2020.

[9] Y. Toor, P. Muhlethaler, A. Laouiti, and A. La Fortelle, "Vehicle ad hoc networks: Applications and related technical issues," *IEEE Commun. Surveys Tuts.*, vol. 10, no. 3, pp. 74–88, 3rd Quart., 2008.

[10] J. Zhao, Q. Li, Y. Gong, and K. Zhang, "Computation offloading and resource allocation for cloud assisted mobile edge computing in vehicular networks," *IEEE Trans. Veh. Technol.*, vol. 68, no. 8, pp. 7944–7956, Aug. 2019.

[11] D. Wu, Y. Zhang, L. Bao, and A. C. Regan, "Location-based crowdsourcing for vehicular communication in hybrid networks," *IEEE Trans. Intell. Transp. Syst.*, vol. 14, no. 2, pp. 837–846, Jun. 2013.

[12] D. Wu, D. I. Arkhipov, Y. Zhang, C. H. Liu, and A. C. Regan, "Online war-driving by compressive sensing," *IEEE Trans. Mobile Comput.*, vol. 14, no. 11, pp. 2349–2362, Nov. 2015.
[13] C.-H. Ou, "A roadside unit-based localization scheme for vehicular ad hoc networks," *Int. J. Commun. Syst.*, vol. 27, no. 1, pp. 135–150, Jan. 2014.
[14] F. Ahammed, J. Taheri, A. Y. Zomaya, and M. Ott, "VLOCI: Using distance Measurements to improve the accuracy of location coordinates in GPS-equipped VANETs," in *Proc. Int. ICST Conf. Mobile Ubiquitous Syst.*, 2012, pp. 149–161.
[15] M. Rohani, D. Gingras, V. Vigneron, and D. Gruyer, "A new decentralized Bayesian approach for cooperative vehicle localization based on fusion of GPS and VANET based inter-vehicle distance measurement," *IEEE Intell. Transp. Syst. Mag.*, vol. 7, no. 2, pp. 85–95, Apr. 2015.
[16] J. Zhao and C. Zhao, "Improved hybrid ToA/AoA location algorithm in NLoS environments for wireless sensor networks," *China Commun.*, vol. 8, no. 8, pp. 106–110, Dec. 2011.
[17] A. Khattab, Y. A. Fahmy, and A. Abdel Wahab, "High accuracy GPS-free vehicle localization framework via an INS-assisted single RSU," *Int. J. Distrib. Sensor Netw.*, vol. 11, no. 5, May 2015, Art. no. 795036.
[18] J. Zhao, L. Li, H. Zhang, and Y. Gong, "Signal path reckoning localization method in multipath environment," *China Commun.*, vol. 14, no. 3, pp. 182–189, Mar. 2017.
[19] J. Zhao, H. Zhang, and R. Ran, "Distance geometry-based wireless location algorithms in cellular networks with NLOS errors," *KSII Trans. Internet Inf. Syst.*, vol. 9, no. 6, pp. 2132–2143, Jun. 2015.
[20] A. Abolfathi Momtaz, F. Behnia, R. Amiri, and F. Marvasti, "NLOS identification in range-based source localization: Statistical approach," *IEEE Sensors J.*, vol. 18, no. 9, pp. 3745–3751, May 2018.
[21] L. Li, F. Yang, and Z. Deng, "Non-line-of-sight node localization based on firefly algorithm," in *Proc. 8th Int. Conf. Intell. Control Inf. Process. (ICICIP)*, Nov. 2017, pp. 325–328.
[22] S.-H. Kong and S.-Y. Jun, "Cooperative positioning technique with decentralized malicious vehicle detection," *IEEE Trans. Intell. Transp. Syst.*, vol. 19, no. 3, pp. 826–838, Mar. 2018.
[23] K. Lim, K. M. Tuladhar, and H. Kim, "Detecting location spoofing using ADAS sensors in VANETs," in *Proc. 16th IEEE Annu. Consum. Commun. Netw. Conf. (CCNC)*, Las Vegas, NV, USA, Jan. 2019, pp. 1–4.
[24] T. W. Chim, S. M. Yiu, L. C. K. Hui, and V. O. K. Li, "Security and privacy issues for inter-vehicle communications in VANETs," in *Proc. 6th IEEE Annu. Commun. Soc. Conf. Sensor, Mesh Ad Hoc Commun. Netw. Workshops*, Rome, Italy, Jun. 2009, pp. 1–3.
[25] K. M. A. Alheeti, A. Gruebler, and K. D. McDonald-Maier, "An intrusion detection system against malicious attacks on the communication network of driverless cars," in *Proc. 12th Annu. IEEE Consum. Commun. Netw. Conf. (CCNC)*, Las Vegas, NV, USA, Jan. 2015, pp. 916–921.
[26] S. Yan, R. Malaney, I. Nevat, and G. W. Peters, "Location verification systems for VANETs in rician fading channels," *IEEE Trans. Veh. Technol.*, vol. 65, no. 7, pp. 5652–5664, Jul. 2016.
[27] T. Leinmüller, C. Maihöfer, E. Schoch, and F. Kargl, "Improved security in geographic ad hoc routing through autonomous position verification," in *Proc. 3rd Int. Workshop Veh. Ad Hoc Netw. (VANET)*, Sep. 2006, pp. 57–66.
[28] X. Xue, N. Lin, J. Ding, and Y. Ji, "A trusted neighbor table based location verification for VANET routing," in *Proc. IET 3rd Int. Conf. Wireless, Mobile Multimedia Netw. (ICWMMN)*, Beijing, China, Jan. 2010, pp. 1–5.
[29] P. Mahalanobis, "On the generalized distance in statistics," *Proc. Nat. Inst. Sci. India*, vol. 12, no. 1, pp. 49–55, 1936.

JUNHUI ZHAO (Senior Member, IEEE) received the M.S. and Ph.D. degrees from Southeast University, Nanjing, China, in 1998 and 2004, respectively. From 1998 to 1999, he worked with the Nanjing Institute of Engineers, ZTE Corporation. He worked as an Assistant Professor with the Faculty of Information Technology, Macao University of Science and Technology, in 2004, where he was an Associate Professor, till 2007. He was also a Short Term Visiting Scholar with Yonsei University, South Korea, in 2004. In 2008, he joined Beijing Jiaotong University as an Associate Professor, where he is currently a Professor with the School of Electronics and Information Engineering. From 2013 to 2014, he was a Visiting Scholar with Nanyang Technological University, Singapore. Since 2016, he has been with the School of Information Engineering, East China Jiaotong University. His current research interests include wireless and mobile communications and the related applications, which contain 5G mobile communication technology, high-speed railway communications, vehicle communication networks, wireless localization, and cognitive radio.

YINGHAO ZHANG received the B.Eng. degree in communication engineering from East China Jiaotong University, Nanchang, China, in 2018. He is currently pursuing the M.S. degree with Beijing Jiaotong University, Beijing. His research interests include wireless localization and non-line-of-sight detection.

SHANJIN NI received the B.Eng. degree in communication engineering from the China University of Geosciences, Wuhan, China, in 2014. He is currently pursuing the Ph.D. degree with Beijing Jiaotong University, Beijing. His research interests include massive MIMO communications, deep learning, and optimization techniques.

QIUPING LI received the B.Sc. degree in electronic information science and technology from China West Normal University, Sichuan, China, in 2015. She is currently pursuing the Ph.D. degree in communication and information systems with Beijing Jiaotong University, Beijing, China. Her research interests include heterogeneous cellular networks, vehicular networks, mobile edge computing, resource allocation, and optimization techniques.